NANO-MICRO LETTERS ARTICLE
www.nmletters.org

The Influence of Morphology on Photo-catalytic Activity and Optical Properties of Nano-crystalline ZnO Powder

Javad Moghaddam[1,*], Sara Mollaesmail[1], Saeed Karimi[2]

(Received 20 September 2012; accepted 29 October 2012; published online 10 November 2012.)

Abstract: ZnO nano-particles were synthesized via an ammonical ammonium carbonate solution by precipitation method in presence of some additives such as urea, oleic and stearic acid. The morphology and crystallinity of the obtained zinc oxide particles depend critically on the type of additive which was used. Additives also affected the crystal orientation of precipitate nano-particles. SEM, XRD, BET and UV-visible were used to characterize morphology, microstructure, specific surface area and optical properties of the products. Photo-catalysis properties of the as-prepared ZnO powders were evaluated by degradation of methyl red (acid red) in aqueous solution exposed to UV-light. Results suggested a close relationship among the morphology, size and surface area on photo-catalysis and optical properties of the particles. The widest E_g value (3.56 eV), highest degradation and decolorization efficiency (99%) were obtained from a sample with the smallest grain size (largest surface area) which were used urea as an additive.
Keywords: Nano-particles; ZnO; Precipitation method; Optical properties; Photocatalytic activity

Citation: Javad Moghaddam, Sara Mollaesmail and Saeed Karimi, "The Influence of Morphology on Photo-catalytic Activity and Optical Properties of Nano-crystalline ZnO Powder", Nano-Micro Lett. 4 (4), 197-201 (2012). http://dx.doi.org/10.3786/nml.v4i4.p197-201

Introduction

ZnO is normally an n-type semiconductor with a wide and direct band gap of 3.37 eV and a large exciton binding energy of 60 meV [1-4]. The structural and optoelectronic properties of semiconductors strongly influenced by their morphology, chemical composition, particle size distribution, environmental condition and fabrication processes [5, 6]. Among various semiconductors, zinc oxide has drawn much attention, because of their interest in fundamental study and also their applied aspects such as in solar energy conversion, varistors, luminescence, photo-catalysis, electrostatic dissipative coating and finally chemical sensors [7-9].

It is evident that the desired chemical and physical properties, and particularly the optical properties and photo-catalytic activity strongly related to the particle sizes and shapes of ZnO powders [10]. In recent years, many researchers have reported that ZnO powders have a more powerful photo-catalytic reaction rather than TiO_2, because ZnO powders can absorb larger fraction of the solar spectrum than TiO_2 powders can. When illuminated with some light source, these semiconductors generate electron–hole pairs, with electrons promoted to the conduction band and leaving positive holes in the valence band. The generated electron–hole pairs initiate a complex series of chemical reactions involving vestigial dye pollutants adsorbed at the surface of the semiconductors that might result in the complete degradation of the adsorbents. For this reason, many

[1]Materials and Metallurgical Engineering Department, Advanced Materials Research Center, Sahand University of Technology, P.O. Box: 51335-1996, Tabriz, Iran
[2]School of Metallurgy and Materials Engineering, University of Tehran, P.O. Box 14395-553, Tehran, Iran
*Corresponding author. Tel.: +98 412 344 3802; Fax: +98 412 344 3443. E-mail: moghaddam@sut.ac.ir; hastyir@yahoo.com

researchers have focused on the synthesis of different morphologies of ZnO powders due to the fact that they displayed the unique properties. Also surface areas and surface defects play an important role in the photocatalytic activities of semiconductors. The synthesis of ZnO photo-catalyst with large surface areas would be of great significance [11, 12].

In this study ZnO nano-particles that were obtained via an ammonical ammonium carbonate zinc aqueous solution precipitation with additives such as Urea, Oleic and Stearic acid were used for characterization. The effects of additives upon the structure and morphology, and also those of particles size, shapes and surface areas on the optical properties and photocatalytic activity were investigated.

Experimental

Preparation of ZnO photo-catalyst

Because of achieving nano-scale particles production from precipitation method, so it needs a homogeneous nucleation from a super-saturation solution. Therefore, at the first step for obtaining maximum solubility condition of zinc oxide in an ammonical ammonium carbonate solution, solubility test was performed. Primary tests showed that the maximum solubility and most practical condition were achieved at pH=9.5 and T=85℃. For preparation of ZnO photo-catalyst, 500 ml of 2 M ammonium carbonate solution was placed into the beaker. When the beakers content reached its desired temperature (85℃), ammonia was slowly added to adjust pH (9.5). The value of pH was determined by a digital pH-meter (Inolab, model listed 8F93). Zinc oxide was added into the solutions until to reach the saturated solution. In this stage, additive solutions such as urea (S_1), oleic acid (S_2) and steraic acid (S_3) were separately added into the main solution. The point of cloud formation and precipitation were investigated for 150 min. After this time, the precipitates were filtered, rinsed by deionized water, dried at 105℃ for 24 h and finally calcinated at 400℃ for 1 h.

Photo-catalytic test

The photo-catalytic tests were performed at an ambient temperature on the samples for decomposition of methyl red (acid red) solution. A pyrex beaker (250 ml) was used as the photo-reactor vessel. An amount of 0.05 g of ZnO samples was added into 100 ml of 1×10^{-5} M aqueous methyl red solution. The solutions were magnetically stirred in the dark for 30 min, and then they were irradiated by a 250 W high-pressure mercury lamp. At given irradiation intervals (5, 10, 15, 20, 25 min), 3 ml of each aqueous solution was collected and centrifuged to remove the ZnO powders, and then was analyzed by a UV-Vis spectrometer (Shimadzu UV-2550). The concentration of aqueous methyl red solution was determined by monitoring the change in the absorbance centered at 515 nm.

Characterizations

The crystallinity and crystal phases of as-prepared samples were determined by the use of X-ray diffraction (XRD, Philips with Cu-K_α radiation). The morphology of particles was studied by scanning electron microscope (SEM, Philips XL30). The specific surface area of nano-sized ZnO particles was determined by nitrogen absorption Brunauer-Emett-Teller (BET) method. The optical absorption of the sample was carried out by a UV-Vis Spectrophotometer (UV-Vis 2550, Shimadzu).

Results and discussions

Morphology, structural properties, specific surface area

Figure 1 shows XRD patterns of all calcined samples which were precipitated from zinc ammonical solution. All the samples exhibit the same XRD patterns. However, the differences in the relative peak intensities of the diffraction pattern of three samples were observed, which can be associated with a particular orientation for each sample. All the diffraction peaks can be indexed only as a diffraction pattern of a hexagonal wurtzite structure in a good agreement with the JCPDS 36-1451, suggesting that the calcined samples are a pure ZnO phase without any secondary phase [13].

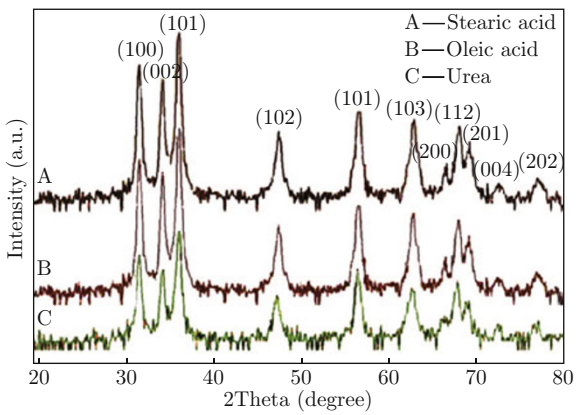

Fig. 1 XRD patterns of all calcined samples.

In order to study the effects of additives on the size of ZnO crystals, the crystallite size of all calcined ZnO powders was calculated from the XRD results by the Scherrer's formula [14]:

$$D = K\lambda/\beta\cos\theta \quad (1)$$

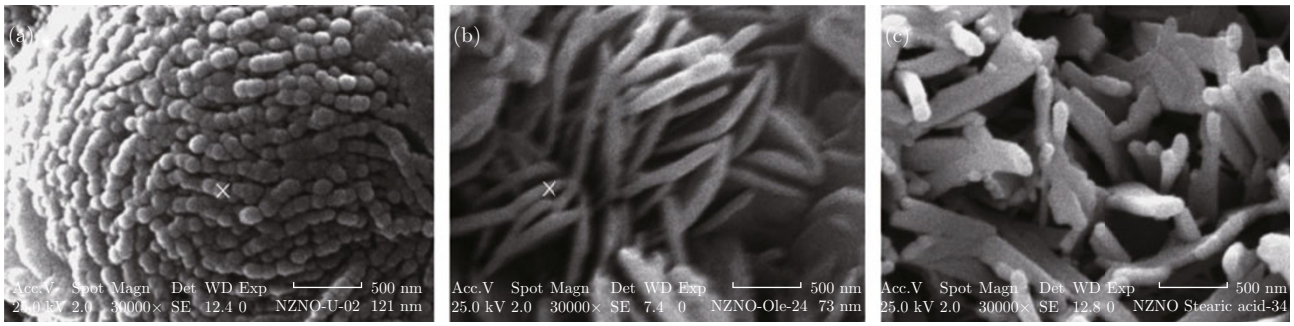

Fig. 2 SEM images of all calcined samples. (a) Urea, (b) Oleic acid, (c) Stearic acid.

where D, K, λ, β and θ are related to the particle diameter, equivalent constant, wavelength of applied X-ray, peak broadening and Bragg angle, respectively. The calculated crystallite size of all calcined ZnO samples is respective 28 nm, 35 nm and 43 nm for $\mathbf{S}_1$, $\mathbf{S}_2$ and $\mathbf{S}_3$ samples.

Figure 2 shows the different morphologies of ZnO nano-powders in the presence of urea, oleic and stearic acid as additives. As it is observed, the morphology of as-prepared zinc oxide powders is greatly influenced by additives which are used.

The obtained results show that the average particles size which were obtained from the analysis of scanning electron microscope images are in a good agreement with the values obtained from the Scherrer's formula. Among three samples, the average particles size of $\mathbf{S}_1$ is the smallest one in comparison with $\mathbf{S}_2$ (72 nm) and $\mathbf{S}_3$ (98 nm) and it is about 60 nm.

The specific surface area of the nano-sized powder samples were obtained from the standard Brunauer-Emmett-Teller (BET) procedure. The BET adsorption isotherm equation can be written as follows:

$$n/n_m = C(p/p_o)/(1-p/p_o)(1+(C-1)p/p_o) \quad (2)$$

where n is the moles of adsorbed gas at p (pressure of adsorbate), C is the BET parameter, n_m is the monolayer capacity in moles, and p_o is the saturation pressure of the adsorbate. The slope and intercept of the linearized form of the equation give the essential parameters used in determining the surface area. After obtained n according to Eq. (2), the S (specific surface area) value of ZnO powder can be calculated using the following equation:

$$S = nN_A a_M \quad (3)$$

where the area that a nitrogen molecular occupies is given by $a_M = 16.2 \times 10^{-20}$ m^2 and Avogadro constant is $N_A = 6.02 \times 10^{23}$ mol^{-1}. As a results, after completing the measurement of BET for the nano-sized ZnO particles, The surface area of S_1, S_2 and S_3 is 82, 69 and 41 m^2/g, respectively.

Band gap evaluation

The dependence of optical band gap on a particle shape and size were studied by some researchers [15]. Figure 3 illustrates the UV-vis absorption spectra of as-prepared samples at room temperature. Figure 3 (A) exhibits absorption spectrum of ZnO nano-particles without any additive, which exhibits absorption edge at 390 nm. Figure 3 (B, C, D) displays the absorption spectrum of samples, which exhibits a sharp absorption edge at 367, 365, 364 nm, respectively.

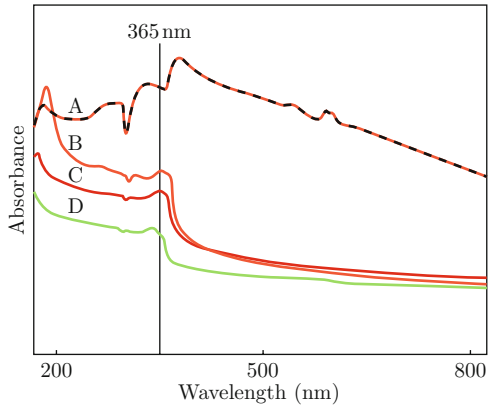

Fig. 3 The UV-vis absorption spectrums of all samples at room temperature.

It is well known that for a crystalline semiconductor the optical absorption near the band edge follows the formula:

$$\alpha h\nu = A(h\nu - E_g)^{n/2} \quad (4)$$

where α is the absorption coefficient, h is the Planck constant, ν is the light frequency, E_g is the band gap, and finally A is a constant. Moreover, among these, n describes the characteristics of the transition in a semiconductor. The value of n for ZnO is 1. The band gap energy (E_g) of samples was determined by extrapolating the linear section of the curve description of the dependence of $(\alpha h\nu)^2$ on the photon energy ($h\nu$) for each of the sample to zero. The plot of $(\alpha h\nu)^2$ versus $h\nu$ based on the direct transition is shown in Fig. 4. The

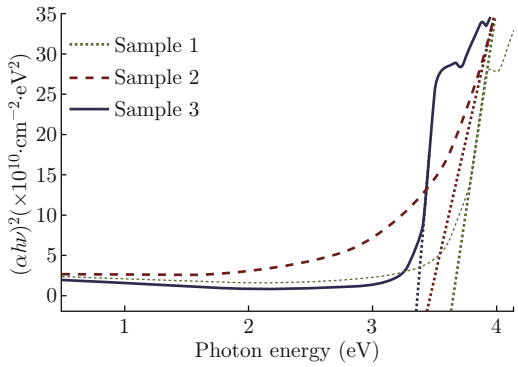

Fig. 4 Relation between $(\alpha h\nu)^2$ and $h\nu$ of different morphological ZnO structure.

band gap shifts toward high amount of energy photon from 3.41 eV to 3.56 eV. The blue shift should be mainly due to the quantum confinement of the ZnO nano-structures. Hence, these three samples have enhanced absorption of ultraviolet radiation which have suitable band gap for photo-catalytic decomposition of organic contaminants under ultraviolet irradiation.

Photo-catalytic activity of ZnO

Figure 5 shows the photo-catalytic efficiency (%) of the different morphological ZnO nano-powders after Hg lamp illumination for 25 min. In the same condition S_1, S_2 and S_3 exhibited 0.99, 0.97 and 0.93 photo-catalytic efficiencies respectively. As it can be seen in Fig. 6, the decolorization efficiency of all samples increased when the irradiation time was increased and the decolorization efficiency was higher than 90% after having irradiated for 20 min. After the suspensions were irradiated by the UV light with energy higher than the bandgap, the electrons (e^-) in the valence band can be excited to the empty conduction band and the holes (h^+) occurred suddenly in the valence band. When the photoelectrons were trapped by oxygen acting as an electronic acceptor, and a superoxide radical anion (O_2^-) was subsequently generated; whereas, the holes were trapped by MR, and in turn these holes acting as an electronic

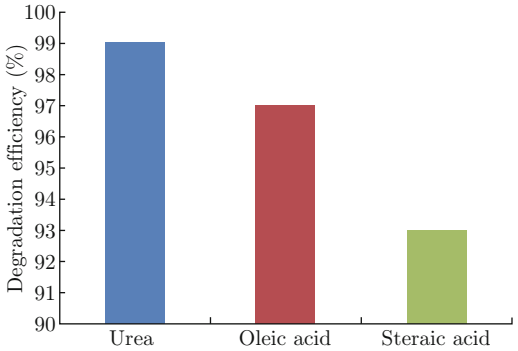

Fig. 5 The photo catalytic efficiency (%) of different morphological ZnO nano powders.

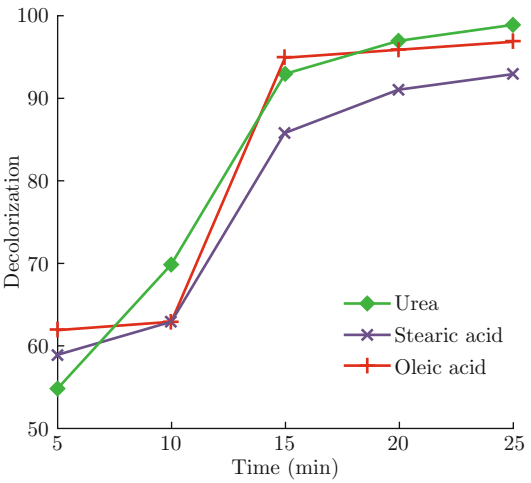

Fig. 6 Relation between decolorization of methyl orange and irradiation time.

donor to oxidize the MR. Considering the decolorization efficiency of S_1, S_2 and S_3 after being irradiated for 20 min, it is evident that the sample with a spherical shape and larger E_g value showed a great powerful oxidation of MR. This is because S_1 has the largest E_g value, the photo induced electrons can stabilize for a long time in the conduction band before coming back to the valence band or we can conclude that the sample with wider E_g value has an appropriate energy potentials of charge carriers that can conduct the redox potential on the sample surface via the separately photo generated electrons and holes [16]. For this reason, the decolorization efficiency of S_1 is higher than those of S_2 and S_3.

Conclusion

The different morphologies of ZnO powders were synthesized via an ammonical ammonium carbonate zinc aqueous solution in presence of some additives such as urea, oleic and stearic acid. As it was shown, the additives can affect the size and morphology of ZnO nano-powders. The powders with different morphologies have different absorption spectra and it will result different values of E_g. A larger E_g value was obtained from a sample with Urea as an additive and it is about 3.56 eV. The photo-catalytic degradation test suggested that ZnO powders showed a great powerful activity in dye degradation of over 99% after having irradiated with the UV light for 20 min. Also the degradation efficiency depended upon the E_g value of samples. The higher efficiency obtained from the sample with larger E_g value because of the retardation of the electron-hole recombination process.

References

[1] K. D. Bhatte, Sh. I. Fujita, M. Arai, A. B. Pandit and B. M. Bhanage, Ultrason. Sonochem. 18

54 (2011). http://dx.doi.org/10.1016/j.ultsonch.2010.06.001

[2] A. K. Singh, Adv. Powder Technol. 21, 609 (2010). http://dx.doi.org/10.1016/j.apt.2010.02.002

[3] Sh. Khameneh Asl, S. K. Sadrnezhaad and M. Kianpourrad, Mater. Lett. 64, 1935 (2010). http://dx.doi.org/10.1016/j.matlet.2010.06.043

[4] L. Lin, H. Watanabe, M. Fuji and M. Takashi, Adv. Powder Technol. 20, 185 (2009). http://dx.doi.org/10.1016/j.apt.2008.08.001

[5] Ch. H. Lu, Y. CH. Lai and R. B. Kale, J. Alloy. Compd. 477, 523 (2009). http://dx.doi.org/10.1016/j.jallcom.2008.10.076

[6] Mingce Long, Jingjing Jiang, Yan Li, Ruqiong Cao, Liying Zhang and Weimin Cai, Nano-Micro Lett. 3, 171 (2011). http://dx.doi.org/10.3786/nml.v3i3.p171-177

[7] R. Hong, T. Pan, J. Qian and H. Li, Chem. Eng. J. 119, 71 (2006). http://dx.doi.org/10.1016/j.cej.2006.03.003

[8] J. S. Park and D. W. Park, Surf. Coat. Tech. 205, S79 (2010). http://dx.doi.org/10.1016/j.surfcoat.2010.04.046

[9] X. Y. Shen, Y. C.Zhai and Y. H. Zhang, T. Nonferr. Metal. Soc. 20, S236 (2010). http://dx.doi.org/10.1016/S1003-6326(10)60046-5

[10] K. G. Chandrappa and T. V. Venkatesha, Nano-Micro Lett. 4, 14 (2012). http://dx.doi.org/10.3786/nml.v4i1.p14-24

[11] R. Y. Hong, J. H. Li, L. L. Chen, D. Q. Liu, H. Z. Li, Y. Zheng and J. Ding, Powder Technol. 189, 426 (2009). http://dx.doi.org/10.1016/j.powtec.2008.07.004

[12] M. Movahedi, E. Kowsari, A. R. Mahjoub and I. Yavari, Mater. Lett. 62, 3856 (2008). http://dx.doi.org/10.1016/j.matlet.2008.05.002

[13] Ch. Ch. Chen, P. Liu and Ch. H. Lu, Chem. Eng. J. 144 , 509 (2008). http://dx.doi.org/10.1016/j.cej.2008.07.047

[14] Y. C. Lee, C. S. Yang, H. J. Huang, S. Y. Hu, J. W. Lee, C. F. Cheng, C. C. Huang, M. K. Tsai and H. C. Kuang, J. Lumin. 130, 1756 (2010). http://dx.doi.org/10.1016/j.jlumin.2010.04.005

[15] S. Suwanboon, P. Amornpitoksuk and N. Muensit, Ceram. Int. 37, 2247 (2011). http://dx.doi.org/10.1016/j.ceramint.2011.03.016

[16] A. Mills and S. L. Hunte, J. Photochem. Photobiol. A 108, 1 (1997). http://dx.doi.org/10.1016/S1010-6030(97)00118-4